Journal of Alloys and Compounds 520 (2012) 202–206

Contents lists available at SciVerse ScienceDirect

Journal of Alloys and Compounds

journal homepage: www.elsevier.com/locate/jallcom

Synthesis, crystal structure and thermal decomposition of $LiCa(AlH_4)_3$

D.M. Liu, Z.X. Qian, T.Z. Si, Q.A. Zhang*

School of Materials Science and Engineering, Anhui University of Technology, Maanshan, Anhui 243002, PR China

ARTICLE INFO

Article history:
Received 12 November 2011
Received in revised form
30 December 2011
Accepted 3 January 2012
Available online 10 January 2012

Keywords:
Lithium–calcium alanate
Synthesis
Crystal structure
Dehydrogenation property

ABSTRACT

Lithium–calcium alanate, $LiCa(AlH_4)_3$, was synthesized by a mechano-chemically activated reaction of $LiAlH_4$ with $CaCl_2$ in a molar ratio of 3:1. The results of X-ray diffraction (XRD) and Fourier transform infrared (FTIR) spectroscopy indicated that the reactants converted entirely into $LiCa(AlH_4)_3$ accompanied with a by-product LiCl after 30 h ball-milling. $LiCa(AlH_4)_3$ crystallized in a hexagonal structure with space group $P6_3/m$ (No. 176), and with cell parameters $a = b = 8.9197(12)$ and $c = 5.8887(7)$ Å. Thermal decomposition of $LiCa(AlH_4)_3$ initiated around 120 °C and proceeded mainly in three steps. The first two steps could be assigned to the formation of CaH_2, LiH and Al, with $LiCaAlH_6$ as a possible intermediate, and the third step was the further formation of some Ca—Al intermetallic phases.

1. Introduction

Since $NaAlH_4$ was discovered to reversibly store hydrogen under moderate conditions by doping with Ti catalysts [1], alkali metal alanates have been extensively investigated for hydrogen storage applications [2–10]. Recently, considerable efforts have further been carried out to develop alkaline-earth metal alanates as potentially promising hydrogen storage materials [11–21]. For example, $Mg(AlH_4)_2$ (~9.3 wt.% H) and $Ca(AlH_4)_2$ (~7.9 wt.% H) can be synthesized not only by wet-chemical or mechano-chemical metathesis reaction of alkali metal alanates with alkaline-earth metal chlorides [11–15] but also by direct ball-milling of AlH_3 with MgH_2 or CaH_2 hydrides [16]. It was found that $Mg(AlH_4)_2$ and $Ca(AlH_4)_2$ might decompose and release hydrogen in two and four steps, respectively [12,14–16], and their dehydrogenation temperature could be reduced by adding catalysts [15,19–21].

Element substitution has been becoming an effective approach to adjust the de-/hydrogenation thermodynamics of conventional metal hydrides and novel complex hydrides [22–25]. Several mixed alanates with two alkali metal cations, such as Na_2LiAlH_6, K_2LiAlH_6 and K_2NaAlH_6, have been synthesized and characterized [26–33]. Among them, Na_2LiAlH_6 and K_2NaAlH_6 take the same cubic ordered perovskite-type structure (space group $Fm\bar{3}m$) [27], while K_2LiAlH_6 has a hexagonal–rhombohedral structure (space group $R\bar{3}m$) [28]. As an extension research of mixed alanates, $LiMg(AlH_4)_3$ and $LiMgAlH_6$ with mixed alkali and alkaline-earth metal cations were also investigated [12,34–37]. It was reported that $LiMg(AlH_4)_3$ and $LiMgAlH_6$ crystallized in space groups $P2_1/c$ and $P321$, respectively, and $LiMgAlH_6$ was the intermediate decomposition product of $LiMg(AlH_4)_3$ [34,35].

In order to explore the mixed calcium alanates and understand their crystal structures and hydrogen storage properties, our recent researches focused on the preparation and characterization of $MCa(AlH_4)_{2+n}$ (M: alkali or alkaline-earth metal) alanates. In the present paper, we report on the mechano-chemical synthesis of lithium–calcium alanate, $LiCa(AlH_4)_3$, with a total hydrogen content of 8.6 wt.%. Furthermore, its crystal structure determined by XRD and thermal decomposition behavior are introduced.

2. Experimental details

2.1. Sample preparation

Commercial $LiAlH_4$ (97%, Alfa Aesar) and anhydrous $CaCl_2$ (99.9%, Alfa Aesar) powders were used as-received. To synthesize $LiCa(AlH_4)_3$, the powders of $LiAlH_4$ and $CaCl_2$ in a molar ratio of 3:1 were mixed manually, and then ball-milled for 10–50 h under argon atmosphere. The ball-milling was performed using a QM-1SP2 planetary mill at a rotation speed of 400 rpm, with stainless steel vials (250 ml in volume) and balls (10 mm in diameter). The ball to powder weight ratio was 30:1. For comparison, $Ca(AlH_4)_2$(+LiCl) was prepared from the mixture of $2LiAlH_4 + CaCl_2$ by the same method described above. For keeping the sample from air-exposure, all the sample handling was carried out in an Ar-filled glove box equipped with a purification system, in which the typical O_2/H_2O levels were below 1 ppm.

2.2. Dehydrogenation property determination

The temperature dependence of dehydrogenation was determined by using a carefully calibrated Sieverts-type apparatus with volumetric method. After evacuation, the sample was heated from ambient temperature to 550 °C at a heating rate of 2 °C min^{-1}. The temperature and the pressure changes in the testing system were digitally recorded; as a result the hydrogen amount desorbed as a

* Corresponding author. Tel.: +86 555 2311891; fax: +86 555 2311570.
E-mail address: zhang03jp@yahoo.com.cn (Q.A. Zhang).

0925-8388/$ – see front matter © 2012 Elsevier B.V. All rights reserved.
doi:10.1016/j.jallcom.2012.01.011

function of temperature can be derived from the gas equation of state modified by a compressibility factor. The weight of the by-product LiCl was not taken into account in calculating the dehydrogenation amounts of the $LiCa(AlH_4)_3$ and $Ca(AlH_4)_2$ samples. The differential scanning calorimetry (DSC) measurement for the $LiCa(AlH_4)_3$ sample was carried out on a Netzsch STA 409 PC/PG unit under argon flow (25 ml min^{-1}) at a heating rate of 10 °C min^{-1}.

2.3. Structure characterization

To evaluate the phase structures of the samples, XRD measurements were carried out using a Rigaku D/Max 2500VL/PC diffractometer with Cu Kα radiation at 50 kV and 200 mA. The XRD samples were loaded and sealed in a special holder that can keep the samples under argon atmosphere in the course of measurement. The software program, TREOR90 [38], was firstly used to index the XRD pattern for $LiCa(AlH_4)_3$; the crystal structure of $LiCa(AlH_4)_3$ was then determined with the EXPO program [39,40]. Based on the structural model, the XRD profile was finally refined by the Rietveld program RIETAN-2000 [41]. FTIR spectra of the $LiCa(AlH_4)_3$ and $Ca(AlH_4)_2$ samples (KBr dispersion) were recorded at ambient condition by using a Nicolet 6700 FTIR spectrometer.

3. Results and discussion

3.1. Synthesis of $LiCa(AlH_4)_3$

$LiCa(AlH_4)_3$ was synthesized by a mechano-chemically activated reaction of $LiAlH_4$ with $CaCl_2$, which can be superficially expressed as follows:

$$3LiAlH_4 + CaCl_2 \rightarrow LiCa(AlH_4)_3 + 2LiCl \quad (1)$$

In order to examine the formation process of $LiCa(AlH_4)_3$, the $3LiAlH_4 + CaCl_2$ mixtures ball-milled for different times were subjected to XRD measurements, and the results are presented in Fig. 1. It can be seen that some additional peaks (indicated by solid square) and the peaks from LiCl emerge in Fig. 1b, indicating the formation of a new phase together with LiCl when ball-milling the $3LiAlH_4 + CaCl_2$ mixture for 10 h. According to reaction (1) and the results of structure analysis (see Section 3.2), the new phase can be determined to be $LiCa(AlH_4)_3$. In order to increase the yield of $LiCa(AlH_4)_3$, the ball-milling time was prolonged to 20 h. As shown in Fig. 1c, the diffraction peaks from $LiCa(AlH_4)_3$ and LiCl are dominant, while those of $LiAlH_4$ and $CaCl_2$ are very weak in the XRD pattern. After ball-milling for 30 h, the diffraction peaks of $LiAlH_4$ and $CaCl_2$ disappear completely, and the product is composed of $LiCa(AlH_4)_3$ and the by-product LiCl (see Fig. 1d). Further increasing the milling time to 50 h, the XRD pattern (Fig. 1e) is hardly changed as compared with Fig. 1d. The results above indicate that $LiCa(AlH_4)_3$ can be readily synthesized by ball-milling the $3LiAlH_4 + CaCl_2$ mixture, and reaction (1) can proceed completely after 30 h ball-milling.

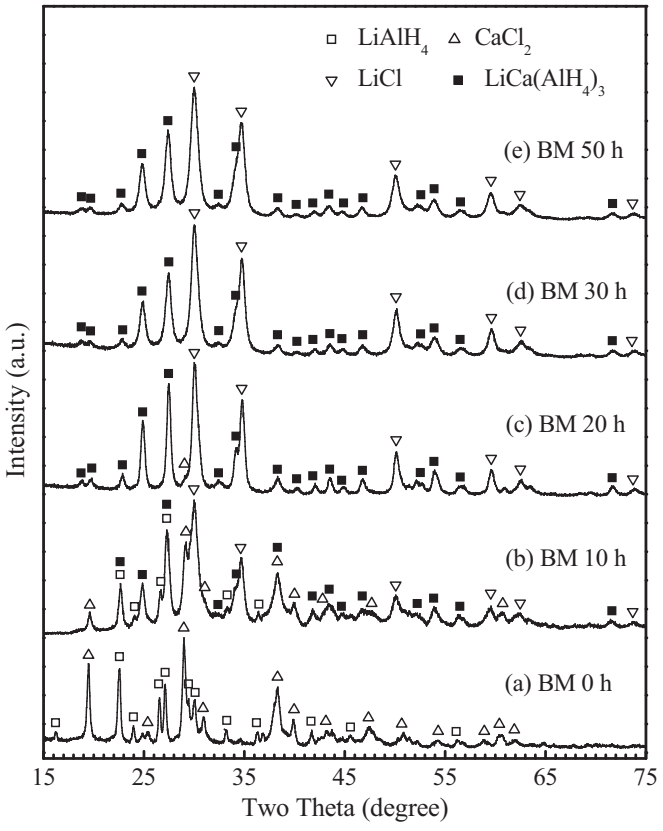

Fig. 1. XRD patterns of $3LiAlH_4 + CaCl_2$ mixtures ball-milled for different times.

To further confirm the formation and give more structural information of $LiCa(AlH_4)_3$, FTIR spectrum of the $3LiAlH_4 + CaCl_2$ mixture after 30 h ball-milling was collected and presented in Fig. 2. For comparison, the FTIR spectrum of the $Ca(AlH_4)_2$ sample prepared by ball-milling $2LiAlH_4 + CaCl_2$ mixture for 30 h is also given in Fig. 2, which shows a Al—H stretching vibration frequency (1800 cm^{-1}) agreeing well with that reported elsewhere (1798 cm^{-1} [19]). It can be seen from Fig. 2 that there is a great difference between the IR spectra of $LiCa(AlH_4)_3$ and $Ca(AlH_4)_2$, due to the distinct chemical environment of Al—H bond in these two compounds. On the one hand, the as-synthesized $LiCa(AlH_4)_3$ sample exhibits two active infra-red stretching vibrations of the Al—H bond (1886 and 1819 cm^{-1}). On the other hand, the Al—H stretching vibration frequency for $LiCa(AlH_4)_3$ is larger than that for $Ca(AlH_4)_2$. No bands from $LiAlH_4$ (1757 and 1615 cm^{-1} [42]) can be detected in the IR spectrum of $LiCa(AlH_4)_3$ sample, implying that the starting materials, $3LiAlH_4 + CaCl_2$, have reacted entirely to form $LiCa(AlH_4)_3$ and LiCl after 30 h ball-milling. Such a result is consistent with that obtained from the XRD study.

3.2. Crystal structure of $LiCa(AlH_4)_3$

$LiCa(AlH_4)_3$ crystallized in a hexagonal structure with space group $P6_3/m$ (No. 176), which is different from those of lithium alanate ($LiAlH_4$, monoclinic structure, space group $P2_1/c$ [43]), calcium alanate ($Ca(AlH_4)_2$, orthorhombic structure, space group *Pbca* [44]) and lithium–magnesium alanate ($LiMg(AlH_4)_3$, monoclinic

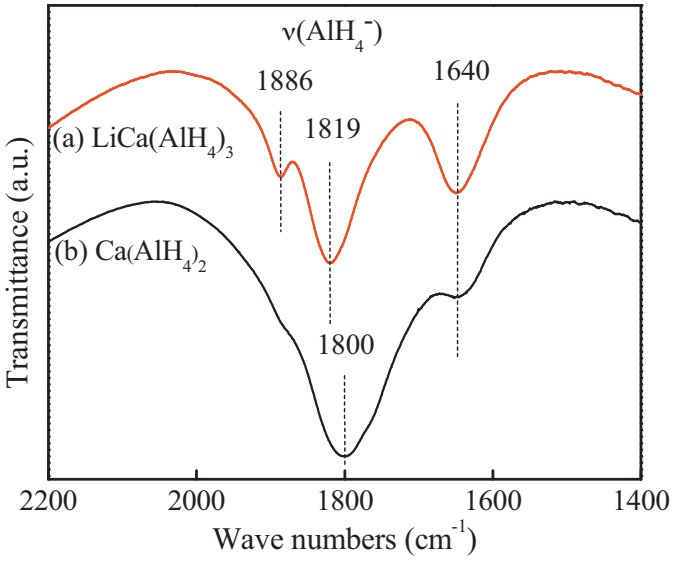

Fig. 2. FTIR spectra of (a) $LiCa(AlH_4)_3$ sample prepared by ball milling the $3LiAlH_4 + CaCl_2$ mixture for 30 h and (b) $Ca(AlH_4)_2$ sample prepared by ball milling the $2LiAlH_4 + CaCl_2$ mixture for 30 h. The band at 1640 cm^{-1} corresponds to water bending vibration [20].

Table 1
Atomic sites, occupancy, coordinates and isotropic thermal parameters for $LiCa(AlH_4)_3$ refined from X-ray powder diffraction data.

Atom	Site	g	x	y	z	B (Å²)
Li	2a	1	0	0	1/4	1.1(2)
Ca	2d	1	2/3	1/3	1/4	2.6(3)
Al	6h	1	0.2805(3)	0.9027(4)	1/4	0.4(4)

Note: Space group $P6_3/m$ (No. 176); cell parameters $a = b = 8.9197(12)$ and $c = 5.8887(7)$ Å; $R_{wp} = 7.28\%$; $R_p = 5.48\%$; $S = 1.69$. The positions of H atoms were not determined.

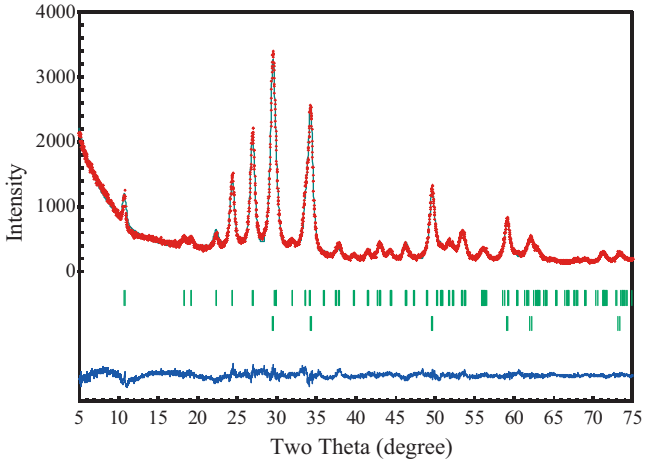

Fig. 3. Rietveld refinement of the XRD pattern for $LiCa(AlH_4)_3$ sample prepared by ball milling the $3LiAlH_4 + CaCl_2$ mixture for 30 h. The vertical bars (from above) indicate the positions of Bragg diffraction for $LiCa(AlH_4)_3$ and LiCl, respectively.

structure, space group $P2_1/c$ [34]). The cell parameters were refined to be $a = b = 8.9197(12)$, $c = 5.8887(7)$ Å and the coordinates of non-hydrogen atoms are listed in Table 1. Fig. 3 shows the observed and calculated XRD patterns of the $LiCa(AlH_4)_3$ sample prepared by ball-milling the $3LiAlH_4 + CaCl_2$ mixture for 30 h. It can be seen that the refined pattern fits the observed data points very well.

The crystal structure of $LiCa(AlH_4)_3$ is illustrated in Fig. 4. Due to the low sensitive of X-ray to hydrogen, the atomic coordinates for H atoms were not determined in the present work and the

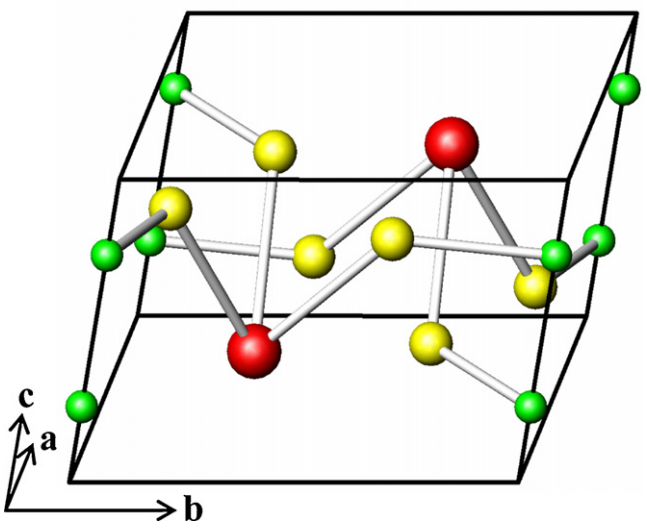

Fig. 4. Crystal structure of $LiCa(AlH_4)_3$ compound. The Li, Ca and Al atoms are, respectively, represented as green, red and yellow spheres. The positions of H atoms were not determined. (For interpretation of the references to color in this figure legend, the reader is referred to the web version of the article.)

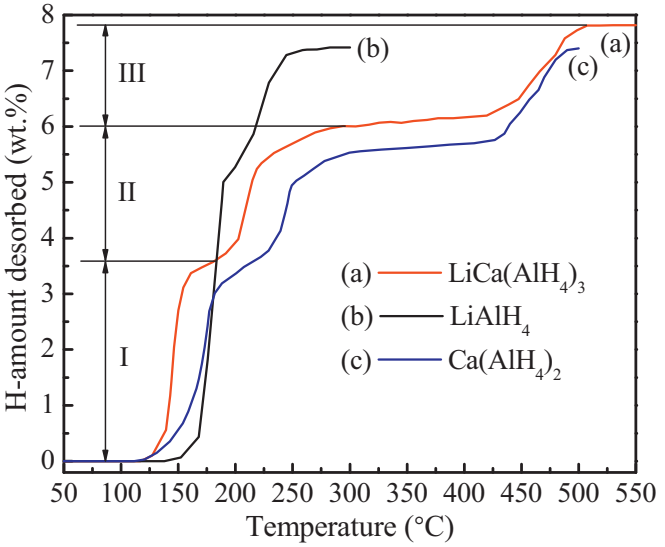

Fig. 5. Hydrogen desorption curves for (a) $LiCa(AlH_4)_3$; (b) $LiAlH_4$ and (c) $Ca(AlH_4)_2$ samples (LiCl is eliminated for calculating the dehydrogenation amounts of $LiCa(AlH_4)_3$ and $Ca(AlH_4)_2$ samples).

characteristics of Al—H, Ca—H and Li—H bonds in $LiCa(AlH_4)_3$ were unknown yet. Even so, it was still found that the Li—Al distance of 3.035 Å is slightly shorter than 3.214–3.415 Å in $LiAlH_4$ [43] and 3.255 Å in $LiMg(AlH_4)_3$ [34], and the Ca—Al distance of 3.774 Å is slightly longer than 3.578 Å in $Ca(AlH_4)_2$ [44]. Further studies on the structure of $LiCa(AlD_4)_3$ by means of neutron diffraction are currently underway.

3.3. Dehydrogenation performance of $LiCa(AlH_4)_3$

Fig. 5 gives the temperature-programmed desorption (TPD) curve for the $LiCa(AlH_4)_3$ sample prepared by ball-milling the $3LiAlH_4 + CaCl_2$ mixture for 30 h. For comparison, the TPD curves for $LiAlH_4$ and $Ca(AlH_4)_2$ are also presented in Fig. 5. It can be seen from Fig. 5 that $LiCa(AlH_4)_3$ starts to release hydrogen around 120 °C, which is similar to that of $Ca(AlH_4)_2$ and is little lower than that of $LiAlH_4$ (140 °C). The thermal dehydrogenation of $LiCa(AlH_4)_3$ is stepwise and can be divided superficially into three steps in the temperature range of 50–550 °C. Step I occurs at about 120–180 °C, with 3.6 wt.% of hydrogen released. The XRD pattern of the product isothermally dehydrogenated at 150 °C is given in Fig. 6b, indicating that a new phase and Al emerge with the disappearance of the starting $LiCa(AlH_4)_3$. Step II starts following Step I and ends at about 300 °C, releasing 2.4 wt.% of hydrogen. The XRD pattern (see Fig. 6c) of the product isothermally dehydrogenated at 300 °C indicates that the characteristic peaks from $CaH_{2-x}Cl_x$, LiH and Al are present, but those from the new phase formed in Step I have disappeared completely. Here, the formation of $CaH_{2-x}Cl_x$ may be the result of that H in CaH_2 was partially substituted by Cl [45]. By analogy with the thermolysis of $LiMg(AlH_4)_3$ and alkali metal alanates [12,33,34], reactions (2) and (3) can be presumed to have happened in Steps I and II, respectively:

$$LiCa(AlH_4)_3 \rightarrow LiCaAlH_6 + 2Al + 3H_2 \quad (2)$$

$$LiCaAlH_6 \rightarrow CaH_2 + LiH + Al + 3/2H_2 \quad (3)$$

According to reactions (2) and (3), the ratio of hydrogen amount desorbed in Step II to Step I should be 2, which is somewhat higher than the measured one (1.5). The reason for the difference in the theoretical and experimental values can be attributed to that reaction (2) is not completely finished in Step I.

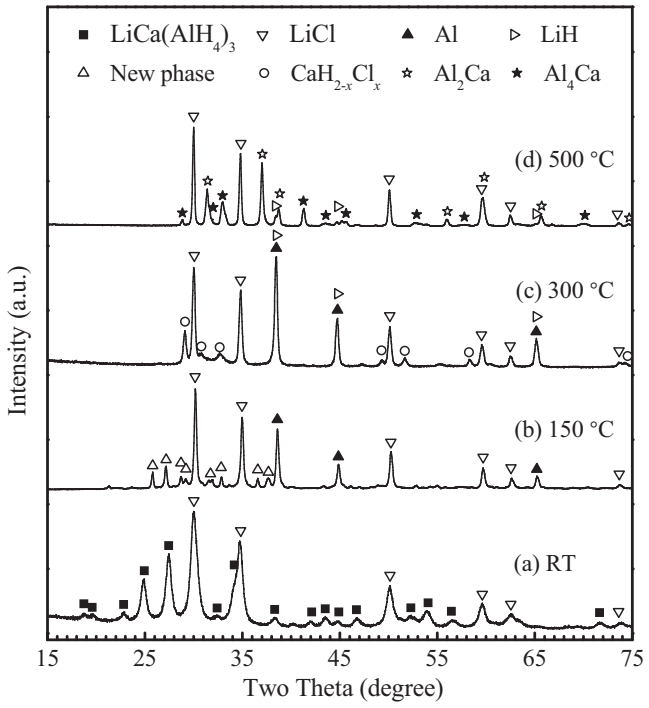

Fig. 6. XRD patterns of $LiCa(AlH_4)_3 + 2LiCl$ mixtures isothermally dehydrogenated for 2 h at different temperatures.

Step III proceeds in the temperature range of 300–510 °C, and releases 1.8 wt.% of hydrogen. As shown in Fig. 6d, the product isothermally dehydrogenated at 500 °C is composed of Al_4Ca, Al_2Ca, LiH and the by-product LiCl. Thus, the third-step dehydrogenation for $LiCa(AlH_4)_3$ can be reasonably expressed as follows:

$$CaH_2 + 3Al \rightarrow 1/2Al_4Ca + 1/2Al_2Ca + H_2 \quad (4)$$

By the combination of reactions (2)–(4), 7.9 wt.% of hydrogen should be released from $LiCa(AlH_4)_3$. This value is in good agreement with the measured one (7.8 wt.%).

To understand the heat effects of the above dehydrogenation steps, Fig. 7 shows the DSC curve of the $LiCa(AlH_4)_3$ sample. It can be seen from Fig. 7 that the first dehydrogenation step of $LiCa(AlH_4)_3$ (corresponding to the first DSC peak) is exothermic, and that Step II

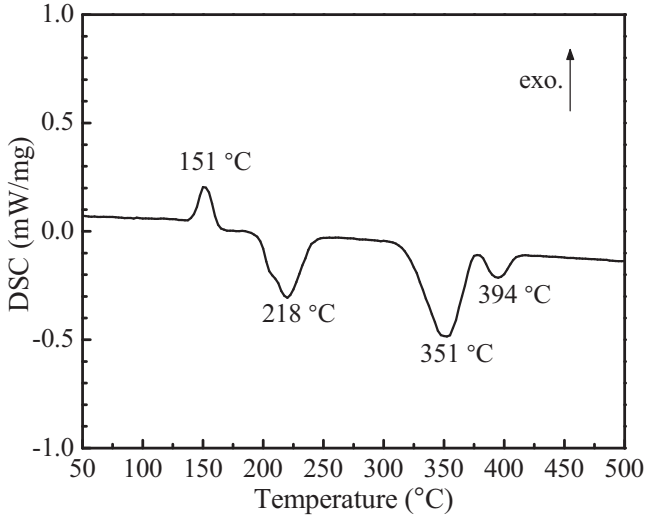

Fig. 7. DSC curve for the $LiCa(AlH_4)_3$ sample prepared by ball milling the $3LiAlH_4 + CaCl_2$ mixture for 30 h.

(the second DSC peak) and Step III (the third and fourth DSC peaks) are endothermic. The results imply that reaction (2) is not likely to occur reversibly, but that reactions (3) and (4) should be thermodynamically reversible. Meanwhile, the post-TPD sample was subjected to hydrogenation at 300 °C under 3 MPa. Only 1.3 wt.% of hydrogen could be reabsorbed, indicating the poor reversibility of $LiCa(AlH_4)_3$.

4. Conclusions

In this paper, the synthesis process, crystal structure and thermal decomposition of $LiCa(AlH_4)_3$ were studied by means of XRD, IR as well as TPD analysis. The results indicated that $LiCa(AlH_4)_3$ could be successfully synthesized by ball-milling the $3LiAlH_4 + CaCl_2$ mixture, and that 30 h of milling duration was sufficient to make the reactants convert entirely into $LiCa(AlH_4)_3$ and LiCl. The structure investigation showed that $LiCa(AlH_4)_3$ had a hexagonal structure in space group $P6_3/m$ (No. 176), with cell parameters $a = b = 8.9197(12)$ and $c = 5.8887(7)$ Å. Hydrogen started to release from $LiCa(AlH_4)_3$ at about 120 °C. The first two dehydrogenation steps of $LiCa(AlH_4)_3$ could be assigned to the formation of CaH_2, LiH and Al, releasing 6.0 wt.% of hydrogen with $LiCaAlH_6$ as a possible intermediate, and the third step was the further formation of some Ca—Al intermetallic phases.

Acknowledgements

This work is financially supported by the National Natural Science Foundation of China (No. 50901001) and the Scientific Research Foundation of Education Department of Anhui Province of China (No. KJ2010A044).

References

[1] B. Bogdanović, M. Schwickardi, J. Alloys Compd. 253–254 (1997) 1.
[2] X.F. Liu, G.S. McGrady, H.W. Langmi, C.M. Jensen, J. Am. Chem. Soc. 131 (2009) 5032.
[3] R.A. Varin, L. Zbroniec, J. Alloys Compd. 506 (2010) 928.
[4] Rafi-ud-din, Z. Lin, P. Li, X.H. Qu, J. Alloys Compd. 508 (2010) 119.
[5] Y.F. Liu, C. Liang, H. Zhou, M.X. Gao, H.G. Pan, Q.D. Wang, Chem. Commun. 47 (2011) 1740.
[6] Y. Li, G. Zhou, F. Fang, X. Yu, Q. Zhang, L. Ouyang, M. Zhu, D. Sun, Acta Mater. 59 (2011) 1829.
[7] P.E. Vullum, M.P. Pitt, J.C. Walmsley, B.C. Hauback, R. Holmestad, J. Alloys Compd. 509 (2011) 281.
[8] X.L. Fan, X.Z. Xiao, L.X. Chen, S.Q. Li, Q.D. Wang, J. Alloys Compd. 509S (2011) S750.
[9] X.P. Zheng, X. Feng, S.L. Liu, J. Alloys Compd. 509 (2011) 5873.
[10] F.E. Pinkerton, J. Alloys Compd. 509 (2011) 8958.
[11] M. Fichtner, C. Frommen, O. Fuhr, Inorg. Chem. 44 (2005) 3479.
[12] M. Mamatha, B. Bogdanović, M. Felderhoff, A. Pommerin, W. Schmidt, F. Schüth, C. Weidenthaler, J. Alloys Compd. 407 (2006) 78.
[13] M. Mamatha, C. Weidenthaler, A. Pommerin, M. Felderhoff, F. Schüth, J. Alloys Compd. 416 (2006) 303.
[14] Y. Kim, E. Lee, J. Shim, Y.W. Cho, K.B. Yoon, J. Alloys Compd. 422 (2006) 283.
[15] K. Komiya, N. Morisaku, Y. Shinzato, K. Ikeda, S. Orimo, Y. Ohki, K. Tatsumi, H. Yukawa, M. Morinaga, J. Alloys Compd. 446–447 (2007) 237.
[16] V. Iosub, T. Matsunaga, K. Tange, M. Ishikiriyama, Int. J. Hydrogen Energy 34 (2009) 906.
[17] D.M. Liu, C.H. Fang, Q.A. Zhang, J. Alloys Compd. 477 (2009) 337.
[18] L. George, S.K. Saxena, Int. J. Hydrogen Energy 35 (2010) 5454.
[19] C.X. Li, X.Z. Xiao, L.X. Chen, K. Jiang, S.Q. Li, Q.D. Wang, J. Alloys Compd. 509 (2011) 590.
[20] X.Z. Xiao, C.X. Li, L.X. Chen, X.L. Fan, H.Q. Kou, Q.D. Wang, J. Alloys Compd. 509S (2011) S743.
[21] C.X. Li, X.Z. Xiao, P.Q. Ge, J.W. Xue, S.Q. Li, H.W. Ge, L.X. Chen, Int. J. Hydrogen Energy (2011), doi:10.1016/j.ijhydene.2011.03.151.
[22] M. Bououdina, D. Grant, G. Walker, Int. J. Hydrogen Energy 31 (2006) 177.
[23] J. Rijssenbeek, Y. Gao, J. Hanson, Q. Huang, C. Jones, B. Toby, J. Alloys Compd. 454 (2008) 233.
[24] I.P. Jain, P. Jain, A. Jain, J. Alloys Compd. 503 (2010) 303.
[25] H. Li, Y. Yan, S. Orimo, A. Züttel, C.M. Jensen, Energies 4 (2011) 185.
[26] X.Z. Ma, E.M. Franco, M. Dornheim, T. Klassen, R. Bormann, J. Alloys Compd. 404–406 (2005) 771.

[27] M.H. Sørby, H.W. Brinks, A. Fossdal, K. Thorshaug, B.C. Hauback, J. Alloys Compd. 415 (2006) 284.
[28] E. Rönnebro, E.H. Majzoub, J. Phys. Chem. B 110 (2006) 25686.
[29] F.H. Wang, Y.F. Liu, M.X. Gao, K. Luo, H.G. Pan, Q.D. Wang, J. Phys. Chem. C 113 (2009) 7978.
[30] Y.F. Liu, F.H. Wang, Y.H. Cao, M.X. Gao, H.G. Pan, Q.D. Wang, Energy Environ. Sci. 3 (2010) 645.
[31] Y.F. Liu, F.H. Wang, Y.H. Cao, M.X. Gao, H.G. Pan, Int. J. Hydrogen Energy 35 (2010) 8343.
[32] X.L. Fan, X.Z. Xiao, L.X. Chen, S.Q. Li, H.W. Ge, Q.D. Wang, J. Mater. Sci. 46 (2011) 3314.
[33] J.E. Fonneløp, O.M. Løvvik, M.H. Sørby, H.W. Brinks, B.C. Hauback, Int. J. Hydrogen Energy 36 (2011) 12279.
[34] H. Grove, H.W. Brinks, R.H. Heyn, F.J. Wu, S.M. Opalka, X. Tang, B.L. Laube, B.C. Hauback, J. Alloys Compd. 455 (2008) 249.
[35] H. Grove, H.W. Brinks, O.M. Løvvik, R.H. Heyn, B.C. Hauback, J. Alloys Compd. 460 (2008) 64.
[36] M.S.L. Hudson, H. Raghubanshi, D. Pukazhselvan, O.N. Srivastava, Int. J. Hydrogen Energy 35 (2010) 2083.
[37] H. Grove, O.M. Løvvik, W. Huang, S.M. Opalka, R.H. Heyn, B.C. Hauback, Int. J. Hydrogen Energy 36 (2011) 7602.
[38] P.E. Werner, L. Eriksson, M. Westdahl, J. Appl. Crystallogr. 18 (1985) 3670.
[39] A. Altomare, M.C. Burla, G. Cascarano, C. Giacovazzo, A. Guagliardi, A.G.G. Moliterni, G. Polidori, J. Appl. Crystallogr. 28 (1995) 842.
[40] A. Altomare, G. Cascarano, C. Giacovazzo, A. Guagliardi, M.C. Burla, G. Polidori, M. Camalli, J. Appl. Crystallogr. 27 (1994) 435.
[41] F. Izumi, T. Ikeda, Mater. Sci. Forum 321–323 (2000) 198.
[42] J.R.A. Fernandez, F.A. Zinsou, M. Elsaesser, X.Z. Ma, M. Dornheim, T. Klassen, R. Bormann, Int. J. Hydrogen Energy 32 (2007) 1033.
[43] B.C. Hauback, H.W. Brinks, H. Fjellvåg, J. Alloys Compd. 346 (2002) 184.
[44] T. Sato, M.H. Sørby, K. Ikeda, S. Sato, B.C. Hauback, S. Orimo, J. Alloys Compd. 487 (2009) 472.
[45] J.Y. Lee, Y.-S. Lee, J.-Y. Suh, J.-H. Shim, Y.W. Cho, J. Alloys Compd. 506 (2010) 721.